Low Temperature Physics/Fizika Nizkikh Temperatur, 2020, v. 46, No. 4, pp. 481–496

Break-junction tunneling spectra of Bi2212 superconducting ceramics: Influence of inhomogeneous *d*-wave-Cooper-pairing and charge-density-wave order parameters

Toshikazu Ekino[1], Alexander M. Gabovich[2], Mai Suan Li[3], Henryk Szymczak[3], and Alexander I. Voitenko[2]

[1]*Graduate School of Integrated Arts and Sciences, Hiroshima University, Higashi-Hiroshima 739-8521, Japan*
E-mail: ekino@hiroshima-u.ac.jp

[2]*Institute of Physics, 46 Nauka Ave., Kyiv 03680, Ukraine*
E-mail: gabovich@iop.kiev.ua
voitenko@iop.kiev.ua

[3]*Institute of Physics, 32/46 Al. Lotników, Warsaw PL-02-668, Poland*
E-mail: masli@ifpan.edu.pl
szymh@ifpan.edu.pl

Received November 25, 2019, published online February 28, 2020

Conductance-voltage characteristics (CVCs) of tunnel break junctions made of $Bi_2Sr_2CaCu_2O_{8+\delta}$ crystals were measured. It was demonstrated that the CVCs have a V-shaped inner gap region, similar to those typical of CVCs for tunnel junctions between *d*-wave superconductors. The CVCs have different forms for different junctions, but all of them reveal weak dip-hump structures outside the inner gap region. Calculations of the tunnel current in the *ab* plane of the break junctions were carried out in the model of the inhomogeneous *d*-wave superconductor partially gapped by charge density waves (CDWs). The averaging of the tunnel current over the statistical distributions of both the superconducting and CDW order parameters was carried out. The theoretical results qualitatively reproduce the behavior of experimental curves. A conclusion was made that tunnel directionality and the statistical distributions of both order are crucial factors governing the observed CVC shapes for break junctions made of high-T_c oxides.

Keywords: superconductivity, charge density waves, electronic inhomogeneity, break-junction tunneling, high-temperature oxides.

To the 80th birthday of Valerij A. Shklovskij

1. Introduction

Break-junction (BJ) tunneling constitutes a powerful probing method for measuring energy gaps in superconductors [1–5]. This *in situ* method is especially helpful when the free surfaces of researched samples may react with the environment, so that in the latter case the results might be unduly influenced, being no more intrinsic ones. Unfortunately, high-T_c oxides are prone to compositional and structural changes, so that *in situ* BJ tunneling measurements are the more so desirable. Nevertheless, not a lot of them have been carried out until now [5–11]. BJ tunneling data and other tunnel or point-contact results reveal not only more or less robust structures in the conductance spectra $G(V)$ — here, V is the bias voltage across the tunnel junction — which may be associated with superconducting gaps, but also additional peak-dip-hump-like features [11–20]. The latter, most probably, are weak manifestations of charge-density waves (CDWs) inherent to quasi-two-dimensional materials including high-T_c superconductors [21–31].

Three main factors may hinder the interpretation of the obtained results. These are (i) the long-standing controversy about the actual symmetry of the superconducting order parameter [32–38], (ii) a possibility that the intrinsic

strong-coupling electron-boson interaction rather than CDWs is the origin of extra humps [39–44], (iii) the character and the size of the gap-like structures (e.g., revealed in tunnel or point-contact spectra) substantially vary even for samples randomly chosen from the same batch [11,40,41,45–53]. It also seems that the CDW-related $G(V)$ peak amplitudes are weaker than it would have been expected in view of the rather large apparent CDW gaps. Therefore, we carried out new BJ experiments on single crystals of Bi-based oxides and theoretically calculated $G(V)$ for inhomogeneous d-wave superconductors with CDWs by averaging tunnel conductance-voltage characteristics (CVCs) over the random distributions of both superconducting and CDW order parameters. The origin of the apparent order parameter distributions (since amplitudes of both are interdependent [54], their distributions are also linked, at least in principle) may be different. For instance, it may be the random oxygen atom occupancy in intrinsically non-stoichiometric oxides [51,55–61], which makes microscopic areas different from one another. The mixed-phase formation in a nominally one-phase superconductor can also effectively scatter gap values, as was demonstrated for intentionally produced mixed-phase whiskers [62]. Of course, the gap randomness can be created not only in the bulk, but in the damaged break-junction areas as well.

The structure of the paper is as follows. In Sec. 2, the results of our break-junction $G(V)$ measurements for a number of $Bi_2Sr_2CaCu_2O_{8+\delta}$ samples are presented. They clearly demonstrate that the discrepancies among the CVCs for junctions made of the "same" oxide are so large that they really need an explanation. Section 3 is devoted to our theory describing tunneling in the ab plane between two pieces of the d-wave superconductors with CDWs. In particular, we show that a possibility for seemingly identical two electrodes to form various electrode configurations in the produced junctions and the corresponding averaging over the superconducting- and CDW-order-parameter amplitudes caused by the microscopic sample disorder may lead to quite different $G(V)$ dependences. Hence, the diversity of experimental results (both ours and obtained by other research groups) can be explained by several factors in the framework of the presented theory. The results of corresponding numerical calculations are presented in Sec. 4. Section 5 contains short conclusions that summarize our analysis.

2. Experimental part

Single crystals of differently doped $Bi_2Sr_2CaCu_2O_{8+\delta}$ samples with slightly different critical temperatures, T_c's, were grown using a standard flux method in the 1-atm air environment [63]. The break junctions were created by cracking the samples at cryogenic temperatures, T, by applying the bending force perpendicularly to the CuO_2 plane. The T_c values resistively determined for various junctions fell within an interval of 86–89 K. The differential CVCs, $G(V)$, were measured with the help of modulation method. Relevant experimental details can be found in Refs. 2, 9. Some of the results obtained are presented in Fig. 1.

The main obstacle to the interpretation or fitting of the experimental dependences $G(V)$ is an annoying background lying beyond the voltages corresponding to the energies of the involved gaps, i.e., Ohm's law was not obeyed outside the gap region. This background — as a rule, it varies with doping and is often approximated as a linear or parabolic curve — has been observed many times [16,41,64–69]. If the background strongly varies on the energy scale that is intrinsic to the studied many-body effects (for instance, superconductivity or CDWs), the background contribution cannot be extracted [70] with the help of the standard nor-

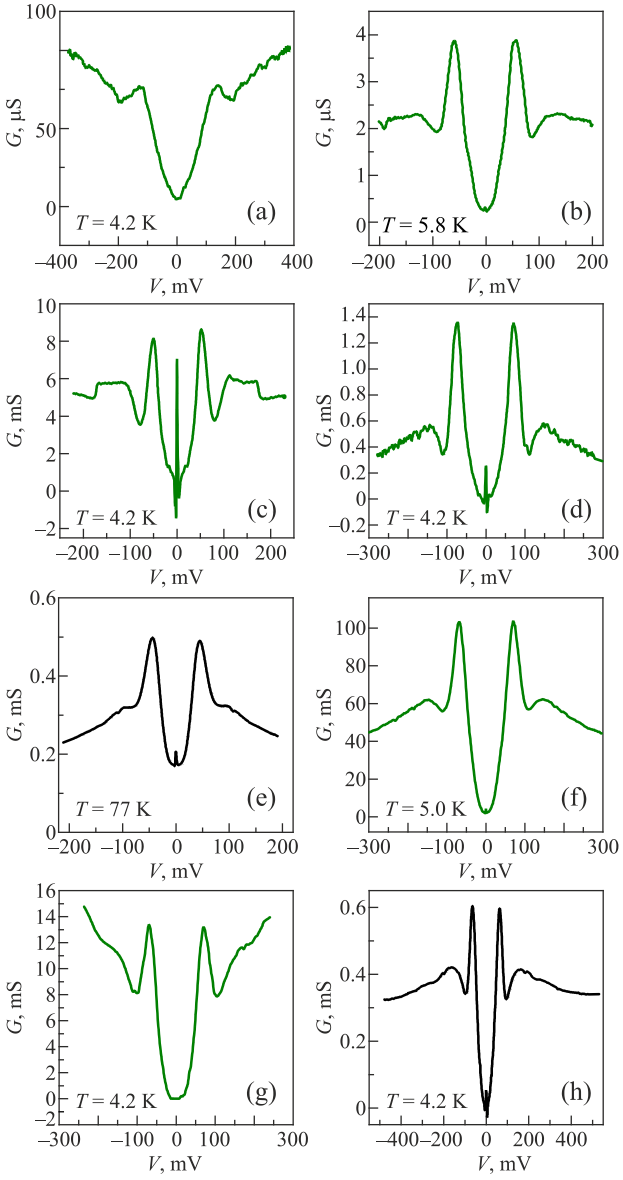

Fig. 1. Experimental conductance-voltage characteristics $G(V)$ of different $Bi_2Sr_2CaCu_2O_{8+\delta}$ break junctions (BJs): (a) to (g) slightly overdoped samples with the critical temperature in the interval of 86–89 K, and (h) an underdoped sample with a critical temperature of about 70 K. The corresponding measurement temperatures are indicated in the panels.

malization rule [71,72]. Although being widely discussed [65,73–75], the normal-state background has no universally accepted explanation yet, and will not be further dealt with in this paper.

Nevertheless, this background does not prohibit from observing that all CVCs possess a characteristic U-shape profile at the zero bias voltage, which is usually associated with the superconducting gap. The limits of the corresponding voltage interval are determined as $eV = \pm 2C_{BCS}T_c$, where e is the elementary charge, and C_{BCS} is one of two well-known proportionality coefficients between the Bardeen–Cooper–Schrieffer (BCS) gap in the weak-coupling approximation and T_c. Specifically, $C_{s\,BCS} = \pi/\gamma \approx 1.764$ if the Cooper pairing is isotropic (*s*-wave) [76], and $C_{d\,BCS} = 2\pi/\gamma\sqrt{e} \approx 2.140$ if it is the *d*-wave one [77]. Here, $\gamma \approx 1.781$ is the Euler constant and $e \approx 2.718$ is the base of natural logarithms.

What is more important for our theory is that the background also does not prohibit from observing CVC sections that lie far beyond this voltage interval and reveal additional CVC peculiarities. Strong-coupling effects can substantially increase the value of C_{BCS} [78–82], but not enough to explain the clear-cut dip-hump structures located at energies far outside the superconducting gap region (see Fig. 1).

There is a popular idea that the additional structure in tunnel CVCs at large biases emerges due to a huge electron-boson coupling with a resonance mode (considered as a Cooper-pairing glue of whatever nature) [26,39–41,43,83–86]. Unfortunately, the dip-hump structure concerned [12–15,17,18,20] cannot be unequivocally associated with the boson interference, because its form varies with doping and is very irregular for tunnel junctions composed of various high-T_c oxides or nominally the same high-T_c superconductor but taken from different batches [11,16,19,67,69,87–90], which is also confirmed by our measurements, depicted in Fig. 1.

On the other hand, there is also a viewpoint that the structure outside the superconducting gap region appears due to some interaction different from the electron-electron attraction stimulated by bosons (phonon or spin-wave), which is responsible for inner (corresponding to the smaller peak-to-peak distance) truly superconducting gapping. In that scenario, the outer smeared gapping (leading to dip-hump features) is associated with the pseudogap-related interaction, charge density waves or spin density waves. All those phenomena are observed in cuprates, with their intensity and even the very existence strongly dependent on doping [21,22,24,25,91–103]. We think, in agreement with a large body of data, that CDWs are the main player competing with superconductivity for the Fermi surface (FS) and partially gapping it, in particular, in the superconducting phase diagram region. If so, it becomes clear why the outer gap structures in the CVCs are located so far away from the inner region: the characteristic temperatures, below which the pseudogap becomes discernible, are much higher than T_c. Moreover, the observed coefficient C_{CDW} in the relationship $eV = \pm 2C_{CDW}T_s$ is much larger (up to 10–13 times [104–108]) than the coefficients $C_{s\,BCS}$ and $C_{d\,BCS}$, although the origin of this discrepancy is unknown and enigmatic in view of the similarity between the gap equations for BCS superconductors [76] and Peierls or similar insulators [109–111] (at least, in the weak-coupling version of the mean-field theories). Here, T_s is the mean-field critical temperature, below which the CDW develops.

Nevertheless, different break junctions displayed in each panel of Fig. 1 reveal non-similar manifestations of the CDW humps. In particular, the latter have different magnitudes and shapes for different CVC branches. The apparent CVC dissimilarity in polarity may result from a number of factors, among which the most probable may be inevitably uncontrolled relative disorientation of the break junction electrodes (more specifically, electrode regions contributing to the tunnel current) and the intrinsic inhomogeneity of high-T_c oxides [11,40,41,45–53,72]. We would like to emphasize that a crucial role for those factors to manifest themselves is played by tunnel directionality. All indicated phenomena are considered in more detail in the next section, where a theoretical model is described.

3. Theoretical description

3.1. Order parameters

Our mean-field theoretical model for *d*-wave superconductors with CDWs on the nested (dielectrized, d) FS sections was suggested earlier [22,54,112–114] (the finiteness of the areas affected by CDWs [115,116] and the smearing of the CDW transition by thermal or quantum fluctuations [93,117–123] lie beyond the applied phenomenological approach). The CDW order parameter $\overline{\Sigma}$ has the *s*-wave symmetry and appears below the critical temperature T_s, which is usually higher than T_c. The superconducting order parameter $\overline{\Delta}(\mathbf{k})$ ($\mathbf{k}$ is the momentum, and the Planck constant $\hbar = 1$) exists on the whole FS, including its d and non-dielectrized (nd) sections. The FS contains $N = 4$ (checkerboard structures) or 2 (unidirectional structures or stripes) d sections. The Hamiltonian of the $d_{x^2-y^2}$-wave superconductor with CDWs (dSCDW) can be found in our previous publication [114]. The parameter $\overline{\Sigma}$ is complex and equals $\Sigma_0(T)e^{i\varphi}$, where φ is the CDW phase. It is $\mathbf{k}$-independent within any of N dielectrically gapped sections in the two-dimensional $\mathbf{k}$ plane. Each of the sections spans the angle 2α. The angle θ is reckoned from the $\mathbf{k}_x$ axis.

In the parent dielectric state, $\Sigma_0(T = 0) = C_{s\,BCS}T_{s0}$ (the Boltzmann constant $k_B = 1$) and $T_s = T_{s0}$, since the CDW state is described by the *s*-wave BCS-like equations [21,124,125]. Hence, in the absence of competing superconductivity, this dielectric order parameter would have the conventional *s*-wave T-dependence. It is instructive to introduce the quantity $\overline{\Sigma}_0(T,\theta) = \Sigma_0(T)f_\Sigma(\theta)$, which spans the whole FS, the angular factor $f_\Sigma(\theta)$ being equal to unity inside and zero outside each *d*-section.

The parent $d_{x^2-y^2}$-wave superconductor (dBCS) [77] is characterized by the order parameter $\Delta_0(0)$ at $T = 0$ and the critical temperature $T_{c0} = C_{d\,BCS}\Delta_0(0)$. The profile $\bar{\Delta}_0(T,\theta)$ in the **k**-space can be also presented in the factorized form $\Delta_0(T) f_\Delta(\theta) \equiv \Delta_0(T)\cos 2\theta$, where $\Delta_0(T)$ is the d-wave superconducting order parameter dependence [77].

When CDWs and superconductivity coexist and compete, the dependences $\Sigma(T)$ and $\Delta(T)$ differ from the parent ones, i.e., $\Sigma_0(T)$ and $\Delta_0(T)$, respectively. Namely, the resulting self-consistent gap equations, which determine $\Sigma(T)$ and $\Delta(T)$ for the given input model parameters ($\Delta_0(0)$, $\Sigma_0(0)$ — they are denoted below as Δ_0 and Σ_0, respectively — α, and N) were derived earlier [22,54,126,127]. The choice of input parameters is arbitrary from the mathematical viewpoint, but we selected them in such a way that the calculated T_c was always lower than T_s, since this is the case of high-T_c oxides and other known CDW superconductors [21–23,97,108,128–131].

On the d FS sections, there appears a combined gap $\bar{D}(T,\theta) = [\Sigma^2(T) + \bar{\Delta}^2(T,\theta)]^{1/2}$ below T_c, whereas an "exclusively superconducting" gap $|\bar{\Delta}(T,\theta)|$ emerges on the remaining nd sections of the FS. Here, the word "exclusively" should be regarded with certain reservations, because the behavior of the superconducting parameter $\Delta(T)$ depends on $\Sigma(T)$.

3.2. Quasiparticle currents in break junctions

In order to substantiate the calculation model, let us first analyze the BJ fabrication procedure. The latter consists of two stages. At the first stage, a dSCDW sample is cracked by applying bending (stretching) forces perpendicularly to the c axis. The gap emerging between the two dSCDW pieces, which now become electrodes, is not a perfect layer with atomically smooth boundaries. Instead, each boundary can be regarded as a fractal-like object: a two-dimensional surface strongly and randomly deformed in the three-dimensional space. Therefore, the orientation of each high-T_c oxide electrode with respect to its nearest boundary with the interelectrode spacing can be arbitrary even if the electrode is not composed of domains with various orientations. At the second stage, those two electrodes are brought closer to each other until the tunnel current appears. In our opinion, not every surface region of each electrode contributes to this current. We believe that, owing to the extremely complicated geometry of the interelectrode gap, there arise only a few current channels between those sites at the surfaces of counter-electrodes where the resistance is the lowest. Those channels are oriented at different angles in the three-dimensional space. As a result, we obtain a random combination of the tunneling channels oriented along the c axis and perpendicularly to it (i.e., in the *ab* plane). The resulting CVCs will demonstrate an average of currents flowing along the c axis and in the *ab* plane, as was shown, e.g., for $Bi_2Sr_2CaCuO_{8+\delta}$ [132]. Another important result consists in that the final CVC should be analyzed as a weighted sum of contributions from a few randomly formed current channels. All the aforesaid brings us to a conclusion that the inherently random character of the BJ fabrication procedure should result in the CVC irreproducibility even for BJs taken from the same crystal batch, which is also confirmed experimentally [133].

We should emphasize that, in this work, we consider quasiparticle BJ tunneling only in the *ab* plane. In this case, tunneling through every of emerged current channels can be illustrated by a corresponding equivalent scheme (see Fig. 2). The orientation of each electrode can be specified by indicating the direction of the corresponding vector $\mathbf{k}_x$. But the orientations of both electrodes (let us call them 0- and V-ones) may not coincide with the current channel orientation [114]. Therefore, the angles γ and γ' showing the orientation of electrodes with respect to the current direction (the vector **n**) may vary within a wide interval $-90° \le (\gamma, \gamma') \le 90°$. Nevertheless, those parameters are fixed for every channel and should not be varied for averaging.

At the same time, the tunnel current is formed in the electrode area that is at least not smaller than the coherence lengths of the both order parameters, Δ and Σ. It means that, due to the microscopic inhomogeneity of high-T_c oxides [11,40,41,45–53,72], the gap averaging of some kind has to affect the overall CVCs. As comes about from the experiment, the CDW order parameter is more fragile than its superconducting counterpart because CDW structures are relatively short range, i.e., do not develop over large areas of the two-dimensional layers [53,93,115,116,134–142]. That is why the apparent spread of CDW gaps are much wider than that of superconducting ones, in particular, in $Bi_2Sr_2CuO_{6+x}$ [72]. However, since the both order parameters are intertwined (in our model, they are the solutions of the same system of equations), their scatters influence each other. Therefore, the spread of amplitudes for both order parameters should be taken into account.

The tunnel current $J(V)$ between the break-junction electrodes was calculated on the basis of the standard tunnel Hamiltonian approach [143]. The expression for $J(V)$

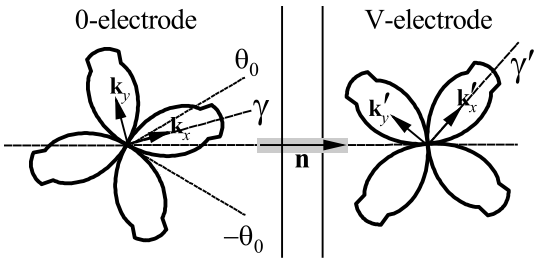

Fig. 2. Two-dimensional (in the *ab* plane) scheme of the BJ between two identical pieces of the d-wave superconductor with charge density waves (dSCDW). The angle $2\theta_0$ describes the directionality cone. The vector **n** shows the current direction. The angles γ and γ' are rotational angles of the dSCDW electrodes reckoned from the vector **n**. See further explanations in the text.

is a functional of the products $G_1 G_2$. Here, G_i is the normal Green's function of the ith electrode. The necessity to take into account Green's function $G_{ib} \propto \Sigma_0(T) f_\Sigma(\theta) e^{i\varphi}$, which is generated by electron-hole pairing and is proportional to the CDW order parameter [110,144], constitutes a peculiarity of the problem and allows non-symmetrical dSCDW junctions to demonstrate non-symmetrical CVCs, whereas the quasiparticle CVCs for currents across non-symmetrical junctions between only conventional *s*-wave [145] or *d*-wave [27,38,114,127,146–148] superconductors are always symmetrical. The tunneling is assumed to be coherent, and directionality effects are made allowance for [114,149–151].

Our calculations include BJ tunneling only in the *ab* plane, so that the angles γ and γ' can be oriented within the sector between the *a* axes of electrodes and the vector **n** oriented normally to the junction plane. This BJ configuration is displayed in Fig. 2. In the framework of the tunnel Hamiltonian method, the following formula for the coherent current $J_{ab}(V)$ across the BJ between two homogeneous electrodes is obtained:

$$J_{ab}(V,\gamma,\gamma') = \frac{1}{2(2\pi)eR}\int_{-\pi}^{\pi} d\theta \cos\theta\, W(\theta) \times$$

$$\times \int_{-\infty}^{\infty} d\omega K(\omega,V,T)\, P(\omega,\theta-\gamma)\, P'(\omega-eV,\theta-\gamma'). \qquad (1)$$

Here, e is the elementary charge. All properties of the tunnel barrier are absorbed into a single phenomenological constant, the barrier resistance R in the normal state. The P-functions describe the densities of electron states in the electrodes. The primed quantities are associated with the V-electrode, whereas the quantities for the 0-electrode are not primed. In particular, for the 0-electrode,

$$P(\omega,\theta) = \frac{\Theta\left(|\omega| - \bar{D}(T,\theta)\right)}{\sqrt{\omega^2 - \bar{D}^2(T,\theta)}} \left[|\omega| + \text{sign}\ \omega \cos\varphi\, \bar{\Sigma}(T,\theta)\right], \qquad (2)$$

where $\Theta(x)$ is the Heaviside step-function. The CDW phase φ is usually pinned at the junction interface and acquires a value of 0 or π (see discussion in Refs. 21, 22). For $P'(\omega - eV, \theta')$, the variable ω in formula (2) has to be changed to $\omega - eV$, and all other parameters, but T, have to be primed. The unconventional term in the brackets of Eq. (2), which is proportional to $\cos\varphi$, is the factor originating from the Green's function G_{ib} [152–154]. For genuinely symmetric junctions, such terms become mutually compensated from equations for the tunnel currents. The multiplier

$$K(\omega,V,T) = \tanh\frac{\omega}{2T} - \tanh\frac{\omega - eV}{2T} \qquad (3)$$

is connected with the temperature-dependent occupation of quasiparticle states in both electrodes. Finally, the multipliers $\cos\theta$ and $W(\theta)$ are associated with the tunnel directionality. This issue is rather important to be briefly considered in a separate section. From the formal point of view, Eq. (1) is a CDW-governed version of the multigap superconductivity applied for many kinds of superconductors [155].

Since our break-junction tunnel experiments were carried at $T \ll (T_c, T_s)$ and the CDW-related peculiarities are better seen at low T, we restricted our calculations to the case $T = 0$.

3.3. Tunnel directionality

The concept of tunnel directionality implies that the contribution of a single quasiparticle into the total tunnel current depends on a number of geometrical factors [112,149–151, 156–158]. One of them becomes relevant if we select the model of coherent tunneling, as was done in this work. It was considered rather in detail in Ref. 38. Briefly speaking, tunneling is allowed only between those sections on the Fermi surfaces of different electrodes that have identical quantum numbers, such as the momentum and the spin. The account of the latter results in the appearance of a factor of $1/2$ in the expression for the tunnel current and do not facilitate calculations. At the same time, the account of the momentum conservation makes it possible to avoid independent integration over each Fermi surface (double integration) and integrate once over a single common variable [the integral over θ in Eq. (1)], which makes calculations much easier.

The origin of other factors giving rise to the appearance of the directional multipliers $\cos\theta$ and $W(\theta)$ in Eq. (1) was discussed earlier while studying the quasiparticle and Josephson tunnel currents [23,112,150,157,159–165]. Namely, the multiplier $\cos\theta$ originates from factors $|\mathbf{v}_{g,nd} \cdot \mathbf{n}|$ and $|\mathbf{v}_{g,d} \cdot \mathbf{n}|$ (here, $\mathbf{v}_{g,nd} = \nabla\xi_{nd}$ and $\mathbf{v}_{g,d} = \nabla\xi_d$ are the quasiparticle group velocities on the corresponding FS sections [160,161]), which are proportional to the number of electron attempts to penetrate through the barrier [166]. Thus, only the normal projection of the quasiparticle motion across the tunnel junction plane is significant [163,166]. The coefficient $W(\theta)$ is the barrier penetration factor [149], which we assume to depend only on θ, so that

$$W(\theta) \approx AY(\theta), \qquad (4)$$

where the coefficient A does not depend on ω in integral (1). That is why the multiplier A can be incorporated into the resistance factor R.

The role of tunnel directionality might be crucial for the BJ tunneling. Indeed, the CVCs are often considered as a tool to determine the energy gaps, whatever their nature [9,167–169]. Nevertheless, the directionality restrictions make the results ambiguous. Specifically, the contributions of those Fermi surface sections that fall outside the "tunneling cone" ($|\theta| > \theta_0$, see Fig. 2) can be effectively "cut off", so that the spectral singularities connected to the FS peculiarities will weakly manifest themselves in the CVCs. The

exact form of the directionality function $Y(\theta)$ is not known, so that we chose the specific $Y(\theta)$ in the form

$$Y(\theta) \sim \begin{cases} \left(\theta_0^2 - \theta^2\right)^2 & \text{if } |\theta| \le \theta_0, \\ 0 & \text{otherwise,} \end{cases} \quad (5)$$

which completely suppresses the contributions of the FS sections falling beyond the tunneling cone θ_0. Therefore, it is clear that the importance of certain FS sections in the CVC formation strongly depends on the orientation of the BJ electrodes.

Since we consider nominally symmetric junctions between the active surface patches of two formally identical electrodes (they may be rotated at different angles γ and γ' with respect to the current channel, so that the "tunneling cone" may "engage" different regions of the Fermi surface in the electrodes), the common parent superconducting gap Δ_0 at $T = 0$ was chosen as the normalization energy scale.

An important result of tunnel directionality consists in that in the case of different electrode orientations, $\gamma \ne \gamma'$, the "tunneling cone" allows non-identical FS sections of electrodes to participate in the formation of tunnel current. Therefore, in this geometry, the junction becomes non-symmetrical *per se*. Furthermore, the availability of CDWs also makes a contribution to the CVC non-symmetricity with respect to the bias voltage sign. Hence, those two factors jointly distort the symmetric character of tunnel CVCs inherent to tunnel junctions with conventional s- and d-wave superconductors.

3.4. Account of the sample inhomogeneity

Let us consider a single tunnel channel. As has been indicated above, the studied tunneling is only nominally symmetric, because the initial (uncracked) dSCDW sample and, as a result, the both dSCDW electrodes are spatially inhomogeneous objects. We may represent the total tunnel current as the sum (integral) of elementary current contributions between physically small homogeneous regions in each electrode. In effect, only the electrode boundary neighborhood with the linear size of about the order parameter coherence lengths contributes significantly to the total current. Evidently, the latter will depend in this case on the specific spatial distribution of inhomogeneities in them, so that the problem will not have a definite universal solution. Therefore, we assume that the contributing regions are large enough to include all possible gap values. In such a way, we formally get rid of the spatial inhomogeneity. Instead, we introduce a model homogeneous object, each elementary volume (domain) of which is a complete ensemble of dSCDWs with a corresponding distribution of individual parent parameters (Δ_0, Σ_0, α), except for N, which is naturally considered to be identical for both electrodes and for all domains in them. Then, the standard procedure is applied: the total tunnel current is a weighted sum of elementary currents (1) between the domains in different electrodes. It is clear that, in the framework of the selected model, the distribution functions of each problem parameter must be identical for both electrodes. Nevertheless, the possible number of parameters for averaging turns out very large: Δ_0, Σ_0, α, and γ for the 0-electrode, and their counterparts Δ_0', Σ_0', α', and γ' for the V-electrode. Each of those parameters should be averaged independently. Therefore, we adopted the following simplifications. Since there is no experimental evidence concerning the spread of the FS dielectrization degree for any specific oxide doping, we considered this parameter to be constant and identical in the both electrodes ($\alpha = \alpha'$). Each of the rotational parameters γ and γ' was assumed to have a corresponding invariant value for all of the each electrode domains.

Thus, the account of sample inhomogeneity was reduced to the averaging over the spreads of the parent order parameters Δ_0 and Σ_0 for each electrode. As a result, the averaging procedure over the electrode parameters required an evaluation of a four-fold, in the general case, integral: one integral like $S_A^{-1}\int_{A_0^-}^{A_0^+} \ldots w_0(A_0)dA_0$ for each parameter A_0 from the set $\{\Delta_0, \Sigma_0, \Delta_0', \Sigma_0'\}$, where $w_0(A_0)$ is its distribution function, $[A_0^-, A_0^+]$ is the interval of its allowed values, and $S_A = \int_{A_0^-}^{A_0^+} w_0(A_0)dA_0$ is the normalizing integral. Surely, if either of the order parameters, $\Delta_0 = \Delta_0'$ or $\Sigma_0 = \Sigma_0'$, is assumed to be fixed in model calculations, the number of required averagings is reduced.

In our earlier researches dealing with the averaging over the parent electrode parameters [148,170], we used the following non-normalized asymmetric bell-shaped distribution weight function $w_0(A_0)$ within the interval $A_0^- \le A_0 \le A_0^+$:

$$w_0(A_0) \sim \begin{cases} \left[\left(\dfrac{A_0 - A_0^m}{A_0^- - A_0^m}\right)^2 - 1\right]^2 & \text{if } A_0^- \le A_0 \le A_0^m, \\ \left[\left(\dfrac{A_0 - A_0^m}{A_0^+ - A_0^m}\right)^2 - 1\right]^2 & \text{if } A_0^m < A_0 \le A_0^+. \end{cases} \quad (6)$$

Note that distribution (6) may be asymmetric with respect to the maximum at A_0^m. For instance, asymmetric CDW gap distributions were observed for overdoped [171] and underdoped [172] $Bi_2Sr_2CaCu_2O_{8+\delta}$, as well as overdoped $Bi_2Sr_{2-x}La_xCuO_{6+\delta}$ [173].

In this work, our calculations were carried out with the upper limit $A_0^+ = A_0^m$ for all parent order parameters. This model implies that the mean-field value of any parent order parameter can be only reduced but not increased by fluctu-

ations [93,121–123,174,175], the proximity effect [176], or the competition with its counterpart [54]. On the other hand, the lower limit A_0^- in illustrative calculations was chosen to equal the following values: A_0^m (so that the parameter A_0 was constant in this case), $A_0^m/2$, and 0. We should recall that the parameter set $\{\Delta_0, \Sigma_0, \Delta_0', \Sigma_0'\}$ is only a parent one. Every elementary tunnel current is not determined by them directly, but via the set of actual parameters $\{\Delta, \Sigma, \Delta', \Sigma'\}$. From this viewpoint, it is of interest to compare the distribution functions for the parent and actual parameter sets.

Below, all energy parameters for dSCDWs are normalized by the parameter Δ_{00}, which corresponds to the value of the parameter $\Delta_0 = \Delta_0^m$ at which the distribution $w_0(\Delta_0)$ has a maximum. The relevant normalized quantities will be denoted in the lower case, i.e., $\delta_0 = \Delta_0/\Delta_{00}$, $\sigma_0 = \Sigma_0/\Delta_{00}$, $\delta = \Delta/\Delta_{00}$, $\sigma = \Sigma/\Delta_{00}$, and so on.

As an example, let us consider the reference case with $N = 4$, $\delta_0 = \sigma_0 = 1$, and $\alpha = 10°$. At $T = 0$, the actual order parameters equal $\delta \approx 0.985$ and $\sigma \approx 0.263$. In Fig. 3, the normalized distribution function of the parent order parameters $w_0(\delta_0, \sigma_0) = w_0(\delta_0) w_0(\sigma_0)$ is compared with the normalized distribution function of the actual order parameters $w(\delta, \sigma)$ for various spreads of parent order parameters. For a better illustration of the complicated character of the dependence $w(\delta, \sigma)$, the corresponding (right) panels were rotated about the w axis, so that the coordinate origin is located at the nearest to the reader point in the (δ_0, σ_0) plane (the dependences $w_0(\delta_0, \sigma_0)$, left panels) and at the leftmost point in the (δ, σ) plane (the dependences $w(\delta, \sigma)$, right panels). Note that, unlike the function $w_0(\delta_0, \sigma_0)$, the function $w(\delta, \sigma)$ cannot be represented in the factorized form, because the parameters δ and σ are interdependent. First of all, attention should be attracted to the appearance of a high "crest" along the δ axis that corresponds to domains with very small or exactly zero σ values ($\sigma \approx 0$). Since the crest height is much larger than the maximum of the $w(\delta, \sigma)$ dependence in the rest of the (δ, σ) plane, the w-axis scale was split into two intervals in each right panel. The appearance of the crest is described well in the framework of our dSCDW theory [54,126]. In particular, it demonstrates that the superconducting pairing, which spans the whole FS, is "more aggressive" in comparison with the partial CDW one in their competition for the FS and can even completely suppress the appearance of CDWs. The fraction of elementary domains with "almost zero σ" that are accumulated in the crest, i.e., the relative volume of the latter, is rather high in all illustrated cases. It means that CDWs do not cover the whole dSCDW volume but exist in the form of separate patches.

From Fig. 3, one can see that the spread of the superconducting order parameter δ_0 plays a more substantial role in the formation of the final $w(\delta, \sigma)$ dependence. In particular, for the illustrated parameter sets, the spread of the parameter σ within the interval [0,1] takes place at any spread of the parent parameter δ_0 (larger that 0.5; evidently, it

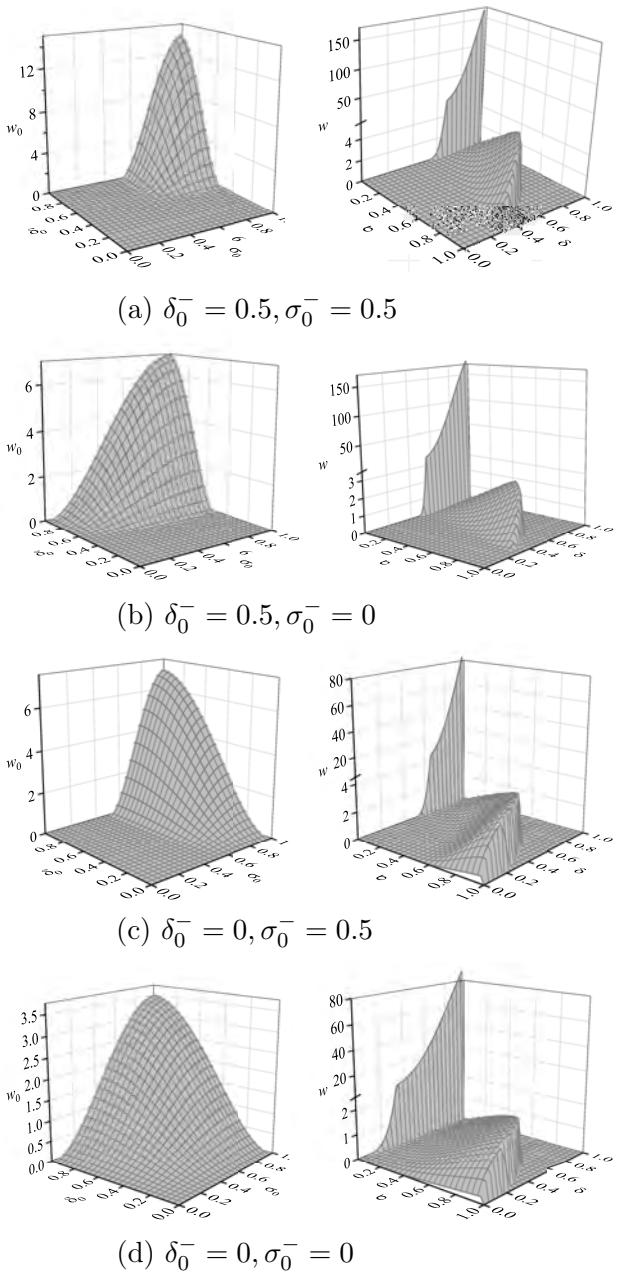

Fig. 3. Distribution functions for the normalized parent — $w_0(\delta_0, \sigma_0)$, left panels — and actual — $w(\delta, \sigma)$, right panels — order parameters for dSCDWs with $N = 4$, $\delta_0^m = \sigma_0^m = 1$, $\alpha = 10°$, and various spreads of the parent order parameters. See further explanations in the text.

can be narrower), irrespective of the spread of the parent parameter σ_0. At the same time, as one can see from panels (a) and (b), even the maximum spread of the parameter σ_0 cannot provide the spread of the parameter δ over the whole interval [0,1] unless the spread of the parameter δ_0 is rather large *per se*. Nevertheless, only the "large" spread of both parent order parameters can lead to the existence of elementary domains with simultaneously small δ and σ values [see wide plateaus around the coordinate origin in panels (a) to (c); the size of those plateaus can be estimated

by the position of the nearest crest edge]. As will be shown below, all those factors clearly manifest themselves in the tunnel CVCs.

The distribution functions $w(\delta,\sigma)$ do not cover the whole story. In particular, they do not contain information about the order parameter distribution within the "tunneling cone". A possibility for two domains participating in tunneling to be disoriented with respect to each other makes the picture even more complicated. This is another argument for the important role of the directionality phenomenon in the formation of CVCs for break junctions fabricated from dSCDWs.

Note that an analogous crest along the δ axis is absent. However, in this work we deal only with the zero temperature $T = 0$. It is clear that if the δ_0 distribution extends down to $\delta_0 = 0$, then, at $T \neq 0$ an analogous crest will arise along the δ axis as well, and it will grow together with the temperature. In our opinion, here, the proper treatment should include the split of superconducting regions in the dSCDW electrodes into domains, similarly to what was suggested for CDWs. The existence of such a patchy structure in cuprates for both the δ and σ distributions is confirmed experimentally [47,72]. For instance, non-superconducting and CDW-free areas (ungapped ones) are always observed in the scanning tunnel microscopy measurements of the high-T_c oxide surfaces [27,53]. At the same time, our calculations presented below show that the qualitative behavior of CVCs taking this possibility into account qualitatively reproduces the experimental data for $Bi_2Sr_2CaCu_2O_{8+\delta}$ obtained in this work.

Some remnants of the account of the spatial electrode inhomogeneity can be detected in that the angular parameter θ in integral (1) was also selected to be random. Hence, the averaging was carried out over five parameters in the general case: δ_0, σ_0, δ_0', δ_0', and θ. But the averaging procedures were different. The inner integral in formula (1) was calculated using the Gauss integration procedure, whereas the averaging over each order parameter, if required, was performed in the framework of the Monte Carlo method.

Our account of the break-junction electrode intrinsic inhomogeneity based on the experimental evidence [11,40,41,45–53,72] is phenomenological. Nevertheless, the gap spread and patchy structures of the oxide surfaces are most probably the consequence at the oxygen random spatial distribution in the non-stoichiometric samples. For instance, the existence of the superconducting puddles in the normal metallic background making the superconducting transition percolative was suggested for $LaAlO_3/SrTiO_3$ or $LaTiO_3/SrTiO_3$ interfaces [177,178]. Earlier, such a scenario was suggested for the bulk superconductivity of the high-T_c oxides [179]. In essence, non-stoichiometry is the basic driving force of the proposed and observed inhomogeneity, being important for both the normal-state conductivity and the formation of the superconducting network.

It is worth noting here that our remark concerning the CVC non-symmetricity as a result of tunnel directionality remains in force. Although the ensembles of gap roses (gap patterns in the two-dimensional $\mathbf{k}$-space) are identical in both electrodes, they are disoriented with respect to each other in the case $\gamma \neq \gamma'$. Accordingly, the "tunneling cone" allows different, in the 0- and V-electrodes, FS sections to participate in tunneling. As a result, the averaging over the parameter distributions that determine those roses should also bring about non-symmetric tunnel CVCs. Taking into account the gap-rose shape (see Fig. 2), it becomes clear that symmetric CVCs can be observed in two cases.

(i) CDWs are absent. This is not impossible, because, as was shown earlier [54,126], d-wave superconductivity is more effective than CDWs in their competition for the FS. In particular, the "CDW re-entrance effect" may arise.

(ii) $\gamma = \pm\gamma'$. The sign "+" corresponds to a genuine symmetric geometry of the junction, whereas the sign "–" describes the antisymmetric one. This scenario is even less probable because of the randomness factor in the formation of break junctions, which was discussed above.

To summarize the theoretical section, the following hypotheses can be put forward in the framework of the presented theory:

— it is highly probable that tunneling in break junctions with dSCDWs takes place through a single or a few rather than plenty of current channels;

— since the dSCDW is an intrinsically inhomogeneous object, one should expect that the peculiarities in tunnel CVCs will be smeared; the degree of this smearing will depend on the degree of inhomogeneity as one of the factors;

— since the formation of tunnel channels has a random character, those channels most probably are established between electrode domains with different order parameter distributions and orientations; moreover, the very CDW pairing leads to the appearance of the current term linear in Σ [180]; as a result, the CVC for a nominally symmetric break junction fabricated from a dSCDW could hardly be expected to be symmetric;

— the phenomenon of tunnel directionality plays an important role in the formation of final CVCs; as a result, various CVC peculiarities can give different contributions (to the extent of their absence) to the cummulative CVCs, which makes the latter rather diverse in shape.

4. Calculations and discussion

4.1. Preliminary remarks

Our model includes several parameters that govern the behavior of CVCs, and it is difficult to run through all their possible combinations. In the absence of parameter spread, the classification of break-junction CVCs and their sufficeently comprehensive account have been made earlier [114]. However, the considered CVCs demonstrated too strong

CDW-related features as compared with the experiment (see, e.g., Refs. 16, 53, 88–90 and the experimental results in Sec. 2). In this work, in the framework of the same approach, we are going to calculate CVCs but in the presence of the order parameter disorder [41,115,116,179,181–186] to adequately describe the smeared structures appropriate to cuprate tunnel junctions.

Let us introduce the dimensionless bias voltage $v = eV / \Delta_{00}$. The dimensionless quasiparticle tunnel current is

$$j = \frac{1}{eR\Delta_{00}} J$$

[see Eq. (1)]. The tunnel conductance $G = dJ / dV$ in the dimensionless form equals $g = R\, dJ / dV = dj / dv$. As was done earlier [127,148,187], the quantity g was calculated as the finite difference

$$g(v) \approx \frac{1}{2\Delta v}\left[j(v+\Delta v) - j(v-\Delta v)\right]. \qquad (7)$$

The differentiation step was selected to equal $\Delta v = 0.001$. The phase φ of the CDW order parameter was chosen to equal π.

4.2. CVCs with the account of disorder

The set of Figs. 4–7 illustrates single-channel tunnel CVCs calculated for break junctions characterized by various inhomogeneities of parent order parameters, with the left electrode oriented along ($\gamma = 0°$) and the right one oriented at different angles γ' with respect to the current direction. The figures demonstrate how the order parameter inhomogeneities reshape CVCs as compared to those for the homogeneous parent dSCDW. In all cases, the latter with the parameters $N = 4$, $\delta_0 = \sigma_0 = 1$, and $\alpha = 10°$ was selected as a reference input. The directionality cone angle was taken to equal $\theta_0 = 45°$.

One should bear in mind that the variety of peculiarities in CVCs appear even in the absence of CDW gapping and is due to the d-wave character of the Cooper pairing studied here and the existence of the directionality cone [114]. CDWs bring additional peculiarities and non-symmetricity to CVCs in non-symmetrical configurations ($\gamma \neq \gamma'$). This can be easily seen in Figs. 5–7. However, CDW-driven features revealed in the absence of disorder are too strong as compared with the experimental data presented in Sec. 2 and in the literature. Thus, the account of the spread was made just in order to reconcile theory and experiment. Indeed, it turned out to be helpful.

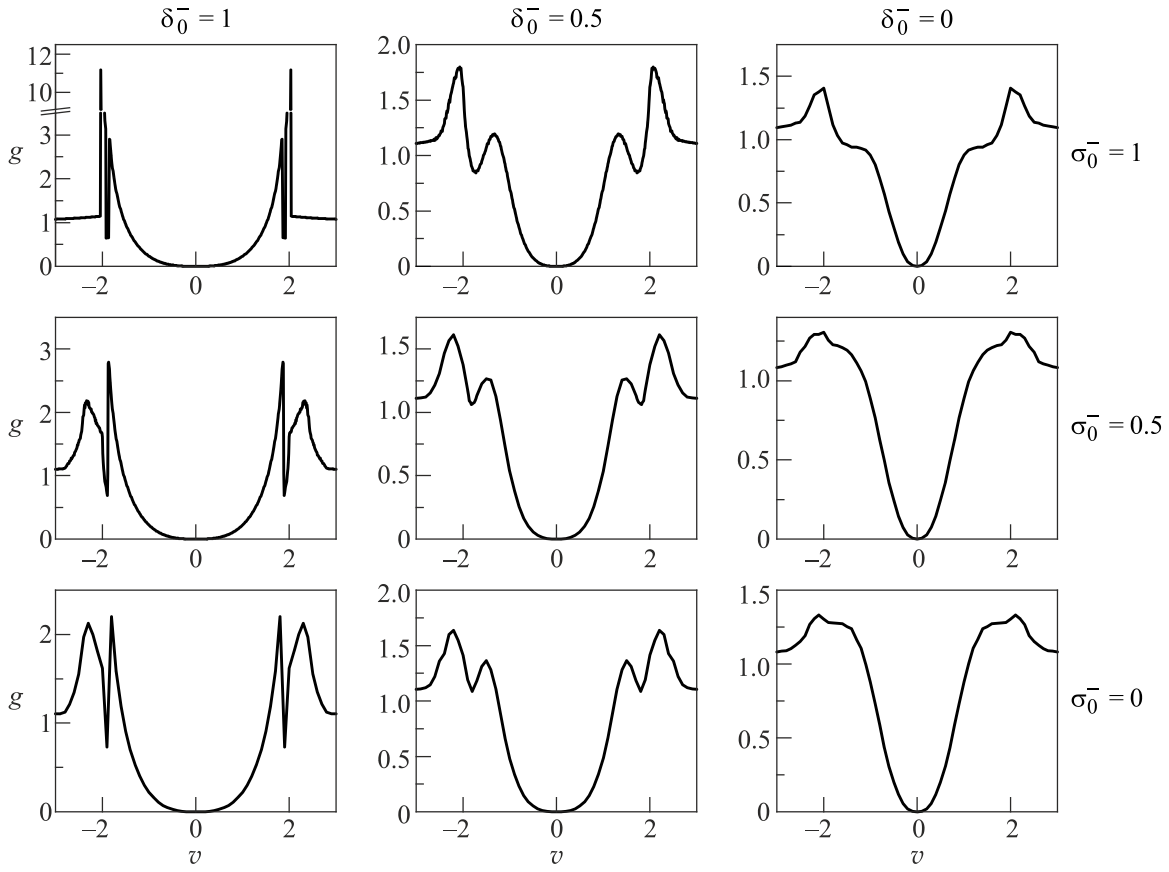

Fig. 4. Normalized conductance-voltage characteristics $g(v)$ calculated for BJs made of dSCDWs with $N = 4$, $\delta_0^m = \sigma_0^m = 1$, $\alpha = 10°$, and various spreads of the parent order parameters. The electrode orientation angles are $\gamma = \gamma' = 0°$. See further explanations in the text.

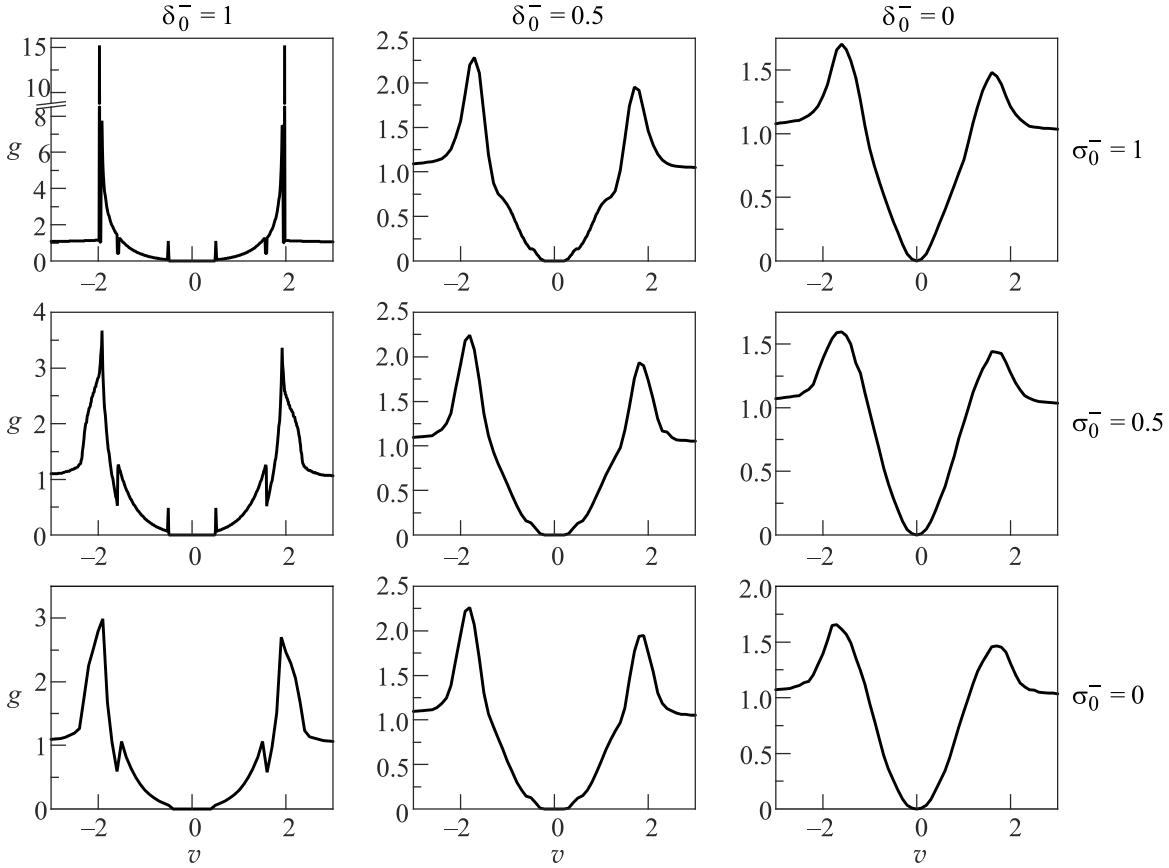

Fig. 5. The same as in Fig. 4, but for $\gamma' = 15°$.

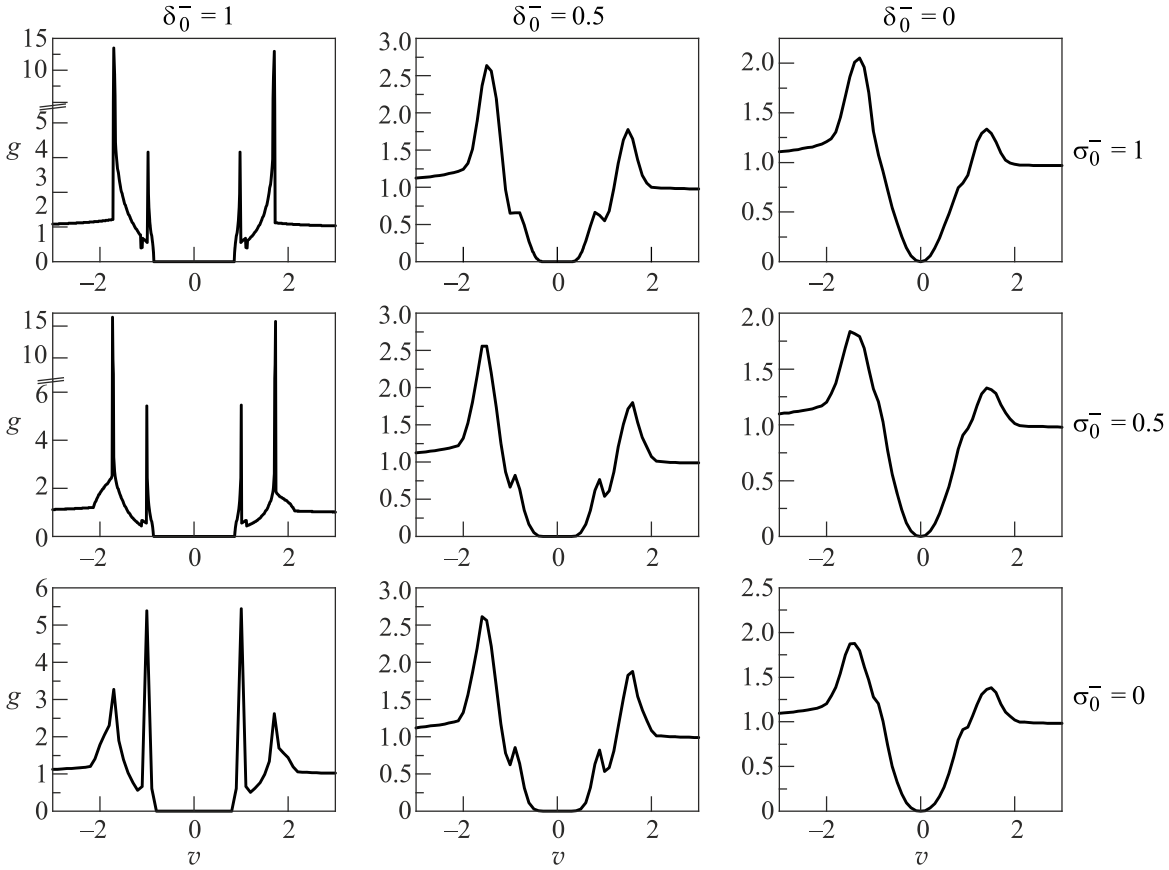

Fig. 6. The same as in Fig. 4, but for $\gamma' = 30°$.

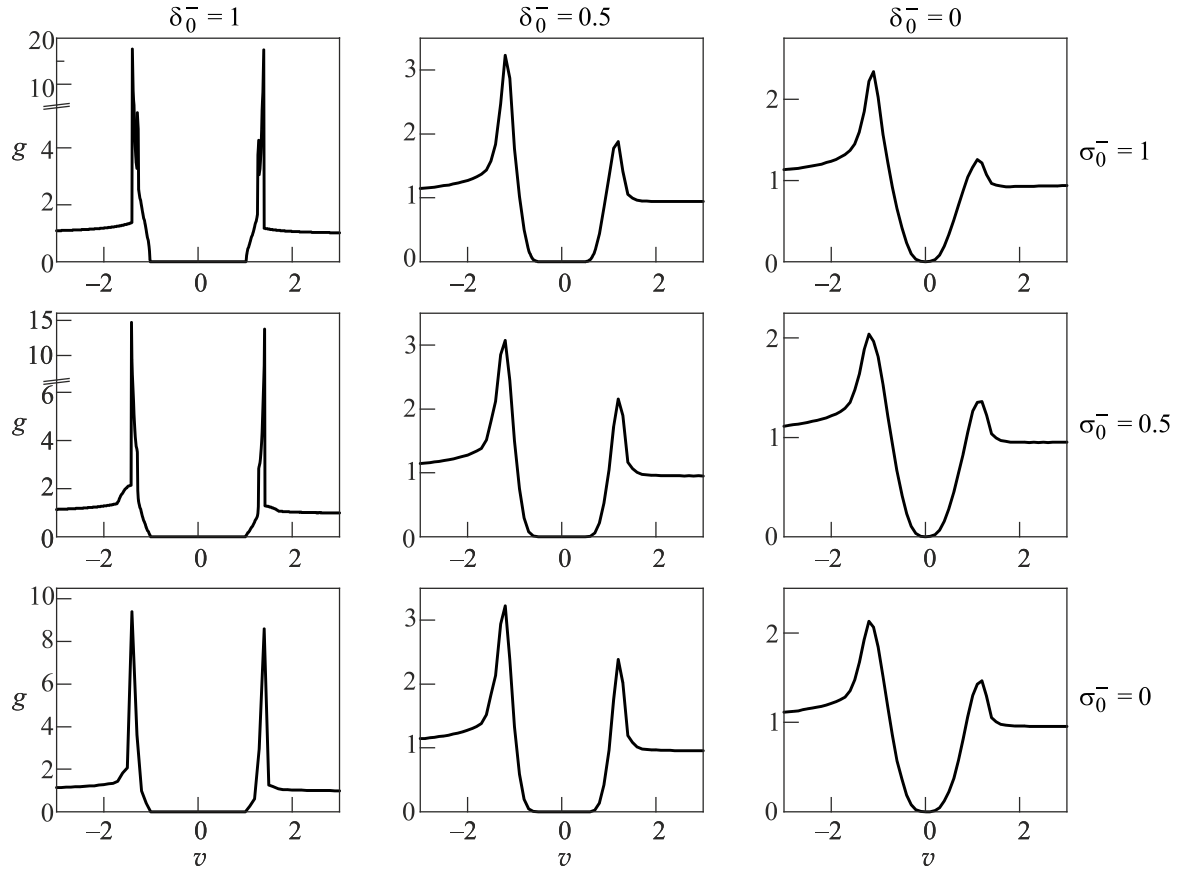

Fig. 7. The same as in Fig. 4, but for $\gamma' = 45°$.

In all cases, the spread of the parameter δ_0 distorts the reference CVCs much stronger than its counterpart of the parameter σ_0. The results of calculations confirm the hypotheses put forward at the end of the previous section. One more conclusion can be made if we compare the calculation and experimental results obtained for the CVC inner gap region (Fig. 1). Here, the matter of concern is both the profile of the gap depression and the ratio between its width and the widths of the peaks at its boundaries. It is evident that the required form and value of this ratio are obtained if the spreads of both order parameters are large enough. Nevertheless, some of experimental CVCs (see, e.g., Fig. 1(g)) testify that a scenario with a broadened depression in the zero-bias neighborhood is also possible, which corresponds to narrower order parameter distributions.

We note that the inner gap region looks like a *d*-wave one for a substantially strong disorder, although in its absence the actual *d*-wave symmetry of the superconducting order parameter can be hidden by the CDW pairing influence. The interplay of both pairings sometimes also leads to the apparently sub-gap features, such as those shown in the middle panels ($\delta_0^- = 0.5$) of Figs. 4 and 6. Such features are similar to experimental data for $YBa_2Cu_3O_{7-\delta}$ obtained by scanning tunneling spectroscopy [69]. One should be careful while interpreting such CVC peculiarities because, as was shown above, the gapping is combined and one cannot unequivocally determine which of the observed CVC features is of a purely superconducting origin.

Finally, we would like to attract attention once more to the role of tunnel directionality in the formation of CVC profiles. Figure 8 demonstrates the set of CVCs calculated

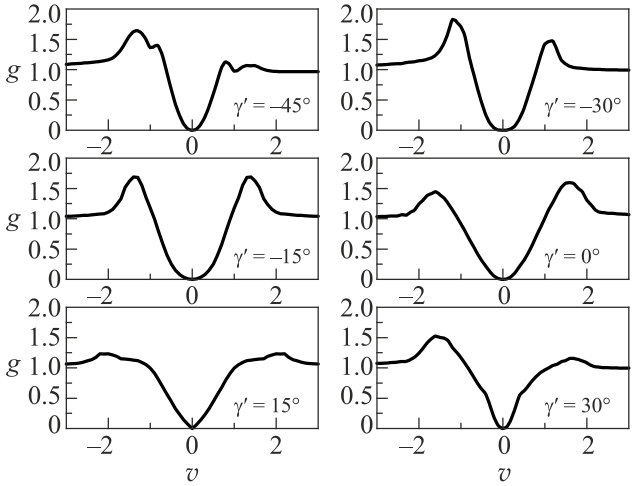

Fig. 8. Normalized conductance-voltage characteristics $g(v)$ calculated for BJs made of dSCDWs with $N = 4$, $\delta_0^m = 1$, $\delta_0^- = 0$, $\sigma_0^m = 1.3$, $\sigma_0^- = 0$, and $\alpha = 10°$. The 0-electrode orientation angle is $\gamma = 15°$, and the V-electrode orientation angles γ' are indicated in the panels. See further explanations in the text.

for the BJ fabricated from a dSCDW with the parameters $N = 4$, $\delta_0^m = \delta_0^+ = 1$, $\delta_0^- = 0$, $\sigma_0^m = \sigma_0^+ = 1.3$, $\sigma_0^- = 0$, and $\alpha = 10°$. In all cases, the 0-electrode is oriented at the constant angle $\gamma = 15°$ with respect to the current direction, whereas the V-electrode orientation γ' varies. Thus, from a formal viewpoint, all analyzed cases are similar, but actually the CVC difference is evident. One can see that, as was said above, CDWs make CVCs non-symmetrical if $\gamma \neq \pm\gamma'$. At the same time, the symmetrical CVCs calculated for $\gamma = \gamma'$ and $\gamma = -\gamma'$ differ from each other, which is a result of the coherent tunneling model.

5. Conclusions

The tunnel conductances $G(V)$ were measured for a number of break junctions made of high-T_c $Bi_2Sr_2CaCu_2O_{8+\delta}$ crystals. The results show that the inner gap regions of the CVCs are partially filled resembling the conventional d-wave-like behavior. At the same time, relatively weak gap-like features exist outside the inner gap region. The appearance of those features is unpredictably irregular. We interpret the minor peculiarities as manifestations of CDWs. Their smeared character is treated as a consequence of the electronic sample inhomogeneity. Hence, the tunnel current is averaged over domains with different values of the superconducting Δ and dielectric Σ order parameters. To confirm our hypothesis, we calculated $G(V)$ in the model of two-dimensional d-wave superconductor partially gapped by CDWs. The wide statistical distribution of order parameters was suggested and included into calculations. The calculated $G(V)$ are quite different for different orientations of the break-junction electrodes. CVCs for non-symmetric electrode orientations are non-symmetric, which is explained by the term in the total current proportional to the CDW order parameter. The CDW-driven strong singularities transform into weak dip-hump structures after the averaging procedure.

Acknowledgments

We thank N-BaRD, Hiroshima University for supplying liquid helium. The work was partially supported by the Project No. 22 of the 2018–2020 Scientific Cooperation Agreement between Poland and Ukraine, the NAS of Ukraine (Grants Nos. 1.4.B-179 and VC-205), the Polish NCN grant 2015/19/B/ST4/02721, and the Japanese Grants-in-Aid for Scientific Research (Nos. 19540370 and 245403770) from JSPS.

1. J. Moreland and J.W. Ekin, *J. Appl. Phys.* **58**, 5888 (1985).
2. T. Ekino, T. Takabatake, H. Tanaka, and H. Fujii, *Phys. Rev. Lett.* **75**, 4262 (1995).
3. R.J.P. Keijsers, O.I. Shklyarevskii, J.G.H. Hermsen, and H. van Kempen, *Rev. Sci. Instrum.* **67**, 2863 (1996).
4. T. Ekino, A. Sugimoto, Y. Sakai, A.M. Gabovich, and J. Akimitsu, *Fiz. Nizk. Temp.* **40**, 1182 (2014) [*Low Temp. Phys.* **40**, 925 (2014)].
5. S.A. Kuzmichev and T.E. Kuzmicheva, *Fiz. Nizk. Temp.* **42**, 1284 (2016) [*Low Temp. Phys.* **42**, 1068 (2016)].
6. D. Mandrus, J. Hartge, C. Kendziora, L. Mihaly, and L. Forro, *Europhys. Lett.* **22**, 199 (1993).
7. R.S. Gonnelli, D. Puttero, G.A. Ummarino, and V.A. Stepanov, *IEEE Trans. Appl. Supercond.* **5**, 2539 (1995).
8. Ya.G. Ponomarev, B.A. Aminov, M.A. Hein, H. Heinrichs, V.Z. Kresin, G. Müller, H. Piel, K. Rosner, S.V. Tchesnokov, E.B. Tsokur, D. Wehler, K. Winzer, A.V. Yarygin, and K.T. Yusupov, *Physica C* **243**, 167 (1995).
9. T. Ekino, Y. Sezaki, and H. Fujii, *Phys. Rev. B* **60**, 6916 (1999).
10. S.I. Vedeneev and D.K. Maude, *Phys. Rev. B* **72**, 144519 (2005).
11. T. Ekino, A.M. Gabovich, M.S. Li, M. Pękała, H. Szymczak, and A.I. Voitenko, *Phys. Rev. B* **76**, 180503 (2007).
12. V.M. Krasnov, A. Yurgens, D. Winkler, P. Delsing, and T. Claeson, *Phys. Rev. Lett.* **84**, 5860 (2000).
13. L. Ozyuzer, J.F. Zasadzinski, C. Kendziora, and K.E. Gray, *Phys. Rev. B* **61**, 3629 (2000).
14. R.M. Dipasupil, M. Oda, N. Momono, and M. Ido, *J. Phys. Soc. Jpn.* **71**, 1535 (2002).
15. Y. Yamada, K. Anagawa, T. Shibauchi, T. Fujii, T. Watanabe, A. Matsuda, and M. Suzuki, *Phys. Rev. B* **68**, 054533 (2003).
16. Ø. Fischer, M. Kugler, I. Maggio-Aprile, and C. Berthod, *Rev. Mod. Phys.* **79**, 353 (2007).
17. P. Das, M.R. Koblischka, H. Rosner, Th. Wolf, and U. Hartmann, *Phys. Rev. B* **78**, 214505 (2008).
18. S.I. Vedeneev, B.A. Piot, and D.K. Maude, *Phys. Rev. B* **81**, 054501 (2010).
19. Y.-F. Lv, W.-L. Wang, H. Ding, Y. Wang, Y. Ding, R. Zhong, J. Schneeloch, G.D. Gu, L. Wang, Ke He, S.-H. Ji, L. Zhao, X.-J. Zhou, C.-L. Song, X.-C. Ma, and Qi-K. Xue, *Phys. Rev. B* **93**, 140504 (2016).
20. T.L. Miller, W. Zhang, J. Ma, H. Eisaki, J.E. Moore, and A. Lanzara, *Phys. Rev. B* **97**, 134517 (2018).
21. A.M. Gabovich, A.I. Voitenko, and M. Ausloos, *Phys. Rep.* **367**, 583 (2002).
22. A.M. Gabovich, A.I. Voitenko, T. Ekino, M.S. Li, H. Szymczak, and M. Pękała, *Adv. Condens. Matter Phys.* **2010**, 681070 (2010).
23. A.M. Gabovich and A.I. Voitenko, *Fiz. Nizk. Temp.* **39**, 301 (2013) [*Low Temp. Phys.* **39**, 232 (2013)].
24. M. Hashimoto, I.M. Vishik, R.H. He, T.P. Devereaux, and Z.-X. Shen, *Nature Phys.* **10**, 483 (2014).
25. A.A. Kordyuk, *Fiz. Nizk. Temp.* **41**, 417 (2015) [*Low Temp. Phys.* **41**, 319 (2015)].
26. M. Hashimoto, E.A. Nowadnick, R.H. He, I.M. Vishik, B. Moritz, Yu He, K. Tanaka, R.G. Moore, D. Lu, Y. Yoshida, M. Ishikado, T. Sasagawa, K. Fujita, S. Ishida, S. Uchida, H.i Eisaki, Z. Hussain, T.P. Devereaux, Z.X. Shen, *Nature Mater.* **14**, 37 (2015).
27. A.M. Gabovich and A.I. Voitenko, *Fiz. Nizk. Temp.* **42**, 1103 (2016) [*Low Temp. Phys.* **42**, 863 (2016)].
28. H.-H. Kim, S.M. Souliou, M.E. Barber, E. Lefrançois, M. Minola, M. Tortora, R. Heid, N. Nandi, R.A. Borzi, G. Garbarino,

A. Bosak, J. Porras, T. Loew, M. König, P.J.W. Moll, A.P. Mackenzie, B. Keimer, C.W. Hicks, and M. Le Tacon, *Science* **362**, 1040 (2018).
29. J. Kačmarčik, I. Vinograd, B. Michon, A. Rydh, A. Demuer, R. Zhou, H. Mayaffre, R. Liang, W. N. Hardy, D. A. Bonn, N. Doiron-Leyraud, L. Taillefer, M.-H. Julien, C. Marcenat, and T. Klein, *Phys. Rev. Lett.* **121**, 167002 (2018).
30. O. Cyr-Choinière, D. LeBoeuf, S. Badoux, S. Dufour-Beauséjour, D.A. Bonn, W.N. Hardy, R. Liang, D. Graf, N. Doiron-Leyraud, and Louis Taillefer, *Phys. Rev. B* **98**, 064513 (2018).
31. X. Li, Y. Ding, C. He, W. Ruan, P. Cai, C.Ye, Z. Hao, L. Zhao, X. Zhou, Q. Wang, and Y. Wang, *New J. Phys.* **20**, 063041 (2018).
32. H. Hilgenkamp and J. Mannhart, *Rev. Mod. Phys.* **74**, 485 (2002).
33. R.A. Klemm, *Philos. Mag.* **85**, 801 (2005).
34. J.R. Kirtley, C.C. Tsuei, Ariando, C.J.M. Verwijs, S. Harkema, and H. Hilgenkamp, *Nature Phys.* **2**, 190 (2006).
35. H. Hilgenkamp, *Supercond. Sci. Technol.* **21**, 034011 (2008).
36. J.R. Kirtley, *C.R. Physique* **12**, 436 (2011).
37. F. Tafuri, L. Galletti, D. Massarotti, and D. Stornaiuolo, *J. Supercond.* **26**, 21 (2013).
38. A.M. Gabovich and A.I. Voitenko, *Fiz. Nizk. Temp.* **43**, 1471 (2017) [*Low Temp. Phys.* **43**, 1172 (2017)].
39. M. Eschrig and M.R. Norman, *Phys. Rev. Lett.* **85**, 3261 (2000).
40. J. Lee, K. Fujita, K. McElroy, J.A. Slezak, M. Wang, Y. Aiura, H. Bando, M. Ishikado, T. Masui, J.-X. Zhu, A.V. Balatsky, H. Eisaki, S. Uchida, and J.C. Davis, *Nature* **442**, 546 (2006).
41. A.N. Pasupathy, A. Pushp, K.K. Gomes, C.V. Parker, J. Wen, Z. Xu, G. Gu, S. Ono, Y. Ando, and A. Yazdani, *Science* **320**, 196 (2008).
42. J.P. Carbotte, T. Timusk, and J. Hwang, *Rep. Prog. Phys.* **74**, 066501 (2011).
43. C. Berthod, Y. Fasano, I. Maggio-Aprile, A. Piriou, E. Giannini, G. Levy de Castro, and Ø. Fischer, *Phys. Rev. B* **88**, 014528 (2013).
44. Y. He, M. Hashimoto, D. Song, S.-D. Chen, J. He, I.M. Vishik, B. Moritz, D.-H. Lee, N. Nagaosa, J. Zaanen, T.P. Devereaux, Y. Yoshida, H. Eisaki, D.H. Lu, and Z.-X. Shen, *Science* **362**, 62 (2018).
45. A.M. Gabovich and A.I. Voitenko, *Phys. Rev. B* **60**, 7465 (1999).
46. V.Z. Kresin, Yu.N. Ovchinnikov, and S.A. Wolf, *J. Supercond.* **14**, 301 (2001).
47. S.H. Pan, J.P. O'Neal, R.L. Badzey, C. Chamon, H. Ding, J.R. Engelbrecht, Z. Wang, H. Eisaki, S. Uchida, A.K. Gupta, K.W. Ng, E.W. Hudson, K.M. Lang, and J.C. Davis, *Nature* **413**, 282 (2001).
48. K.M. Lang, V. Madhavan, J.E. Hoffman, E.W. Hudson, H. Eisaki, S. Uchida, and J.C. Davis, *Nature* **415**, 412 (2002).
49. C. Howald, H. Eisaki, N. Kaneko, M. Greven, and A. Kapitulnik, *Phys. Rev. B* **67**, 014533 (2003).
50. V. Kresin, Yu. Ovchinnikov, and S. Wolf, *Phys. Rep.* **431**, 231 (2006).
51. J.A. Slezak, J. Lee, M. Wang, K. McElroy, K. Fujita, B.M. Andersen, P.J. Hirschfeld, H. Eisaki, S. Uchida, and J.C. Davis, *Proc. Nat. Acad. Sci. USA* **105**, 3203 (2008).
52. H.G. Luo, Y.H. Su, and T. Xiang, *Phys. Rev. B* **77**, 014529 (2008).
53. A. Sugimoto, T. Ekino, A.M. Gabovich, R. Sekine, K. Tanabe, and K. Tokiwa, *Phys. Rev. B* **95**, 174508 (2017).
54. T. Ekino, A.M. Gabovich, M.S. Li, M. Pękała, H. Szymczak, and A.I. Voitenko, *J. Phys.: Condens. Matter* **23**, 385701 (2011).
55. B. Raveau, *Phys. Today* **45**, 53 (1992).
56. S.E. Babcock and J.L. Vargas, *Annu. Rev. Mater. Sci.* **25**, 193 (1995).
57. M. Karppinen and H. Yamauchi, *Mat. Sci. Eng. R* **26**, 51 (1999).
58. R.J. Cava, *J. Am. Ceram. Soc.* **83**, 5 (2000).
59. J. Ayache, *Philos. Mag.* **86**, 2193 (2006).
60. B. Raveau, *Prog. Solid State Chem.* **35**, 171 (2007).
61. R.V. Vovk and A.L. Solovjov, *Fiz. Nizk. Temp.* **44**, 111 (2018) [*Low Temp. Phys.* **44**, 81 (2018)].
62. O. Kizilaslan, M. Truccato, Y. Simsek, M.A. Aksan, Y. Koval, and P. Müller, *Supercond. Sci. Technol.* **29**, 065013 (2016).
63. D.B. Mitzi, L.W. Lombardo, A. Kapitulnik, S.S. Laderman, and R.D. Jacowitz, *Phys. Rev. B* **41**, 6564 (1990).
64. H.L. Edwards, J.T. Markert, and A.L. de Lozanne, *Phys. Rev. Lett.* **69**, 2967 (1992).
65. Ch. Renner and Ø. Fischer, *Phys. Rev. B* **51**, 9208 (1995).
66. S. Kashiwaya and Y. Tanaka, *Rep. Prog. Phys.* **63**, 1641 (2000).
67. J.F. Zasadzinski, in: *Superconductivity. Vol. 2*: *Novel Superconductors*, K.H. Bennemann and J.B. Ketterson (eds.), Springer Verlag, Berlin (2008), p. 833.
68. Th. Jacobs, S.O. Katterwe, H. Motzkau, A. Rydh, A. Maljuk, T. Helm, C. Putzke, E. Kampert, M.V. Kartsovnik, and V.M. Krasnov, *Phys. Rev. B* **86**, 214506 (2012).
69. J. Bruér, I. Maggio-Aprile, N. Jenkins, Z. Ristić, A. Erb, C. Berthod, Ø. Fischer, and C. Renner, *Nat. Commun.* **7**, 11139 (2016).
70. J. Geerk and H.V. Löhneysen, *Phys. Rev. Lett.* **99**, 257005 (2007).
71. W.L. McMillan and J.M. Rowell, in: *Superconductivity*, R.D. Parks (ed.), Dekker, New York (1969), Vol. 1, p. 561.
72. M.C. Boyer, W.D. Wise, K. Chatterjee, M. Yi, T. Kondo, T. Takeuchi, H. Ikuta, and E.W. Hudson, *Nature Phys.* **3**, 802 (2007).
73. J.G. Simmons, *J. Appl. Phys.* **34**, 1793 (1963).
74. J.R. Kirtley and D.J. Scalapino, *Phys. Rev. Lett.* **65**, 798 (1990).
75. J.C. Slonczewski and J.Z. Sun, *J. Magn. Magn. Mater.* **310**, 169 (2007).
76. J. Bardeen, L.N. Cooper, and J.R. Schrieffer, *Phys. Rev.* **108**, 1175 (1957).
77. H. Won and K. Maki, *Phys. Rev. B* **49**, 1397 (1994).
78. J.P. Carbotte, *Rev. Mod. Phys.* **62**, 1027 (1990).
79. E. Schachinger and J.P. Carbotte, *Phys. Rev. B* **43**, 10279 (1991).
80. J. Song and J.F. Annett, *Phys. Rev. B* **51**, 3840 (1995).
81. E. Cappelluti and G.A. Ummarino, *Phys. Rev. B* **76**, 104522 (2007).
82. V.Z. Kresin and S.A. Wolf, *Rev. Mod. Phys.* **81**, 481 (2009).
83. G.-M. Zhao, *Phys. Rev. B* **71**, 104517 (2005).
84. G.-M. Zhao, *Phys. Rev. B* **75**, 214507 (2007).
85. G.-M. Zhao, *Phys. Rev. Lett.* **103**, 236403 (2009).
86. C. Berthod, *Phys. Rev. B* **82**, 024504 (2010).

87. T. Ekino, A.M. Gabovich, Mai Suan Li, M. Pękała, H. Szymczak, and A.I. Voitenko, *Metrology Measurement. Syst.* **15**, 145 (2008).
88. V.M. Krasnov, *Phys. Rev. B* **79**, 214510 (2009).
89. H. Motzkau, T. Jacobs, S.-O. Katterwe, A. Rydh, and V.M. Krasnov, *Phys. Rev. B* **85**, 144519 (2012).
90. H. Kambara, I. Kakeya, and M. Suzuki, *Phys. Rev. B* **87**, 214521 (2013).
91. A.M. Gabovich, A.I. Voitenko, J.F. Annett, and M. Ausloos, *Supercond. Sci. Technol.* **14**, R1 (2001).
92. S. Hüfner, M.A. Hossain, A. Damascelli, and G.A. Sawatzky, *Rep. Prog. Phys.* **71**, 062501 (2008).
93. M. Vojta, *Adv. Phys.* **58**, 699 (2009).
94. K. Fujita**,** A.R. Schmidt, E.-A. Kim, M.J. Lawler, D.-H. Lee, J.C. Davis, H. Eisaki, and S.-I. Uchida, *J. Phys. Soc. Jpn.* **81**, 011005 (2012).
95. T. Yoshida, M. Hashimoto, I.M. Vishik, Z.-X. Shen, and A. Fujimori, *J. Phys. Soc. Jpn.* **81**, 011006 (2012).
96. S. Sachdev, M.A. Metlitski, and M. Punk, *J. Phys.: Condens. Matter* **24**, 294205 (2012).
97. C-W. Chen, J. Choe, and E. Morosan, *Rep. Prog. Phys.* **79**, 084505 (2016).
98. T. Kloss, X. Montiel, V.S. de Carvalho, H. Freire, and C. Pépin, *Rep. Prog. Phys.* **79**, 084507 (2016).
99. P. Cea, *Eur. Phys. J. B* **89**, 176 (2016).
100. N.E. Hussey, J. Buhot, and S. Licciardello, *Rep. Prog. Phys.* **81**, 052501 (2018).
101. I.M. Vishik, *Rep. Prog. Phys.* **81**, 062501 (2018).
102. R.M. Fernandes, P.P. Orth, and J. Schmalian, *Annu. Rev. Condens. Matter Phys.* **10**, 133 (2019).
103. C. Proust and L. Taillefer, *Annu. Rev. Condens. Matter Phys.* **10**, 409 (2019).
104. T. Ekino and J. Akimitsu, *Jpn. J. Appl. Phys.* **26**, Suppl. 26–3, 625 (1987).
105. M. Greenblatt, *Chem. Rev.* **88**, 31 (1988).
106. C. Wang, B. Giambattista, C.G. Slough, R.V. Coleman, and M.A. Subramanian, *Phys. Rev. B* **42**, 8890 (1990).
107. Z. Dai, C.G. Slough, W.W. McNairy, and R.V. Coleman, *Phys. Rev. Lett.* **69**, 1769 (1992).
108. P. Monceau, *Adv. Phys.* **61**, 325 (2012).
109. M.J. Rice and S. Strässler, *Solid State Commun.* **13**, 125 (1973).
110. Yu.V. Kopaev, *Trudy Fiz. Inst. Akad. Nauk SSSR* **86**, 3 (1975).
111. G. Grüner, *Density Waves* in: *Solids*, Addison-Wesley Publishing Company, Reading, Massachusetts (1994), p. 259.
112. A.M. Gabovich, M.S. Li, H. Szymczak, and A.I. Voitenko, *Phys. Rev. B* **87**, 104503 (2013).
113. A.M. Gabovich and A.I. Voitenko, *Physica C* **503**, 7 (2014).
114. T. Ekino, A.M. Gabovich, M.S. Li, H. Szymczak, and A.I. Voitenko, *J. Phys.: Condens. Matter* **29**, 505602 (2017).
115. G. Campi, A. Bianconi, N. Poccia, G. Bianconi, L. Barba, G. Arrighetti, D.K.J. Innocenti, N.D. Zhigadlo, S.M. Kazakov, M. Burghammer, M. v. Zimmermann, M. Sprung, and A. Ricci, *Nature* **525**, 359 (2015).
116. G. Campi and A. Bianconi, *J. Supercond.* **29**, 627 (2016).
117. P.A. Lee, T.M. Rice, and P.W. Anderson, *Phys. Rev. Lett.* **31**, 462 (1973).
118. M.J. Rice and S. Strässler, *Solid State Commun.* **13**, 1389 (1973).
119. S.A. Kivelson, I.P. Bindloss, E. Fradkin, V. Oganesyan, J.M. Tranquada, A. Kapitulnik, and C. Howald, *Rev. Mod. Phys.* **75**, 1201 (2003).
120. E. Fradkin, S.A. Kivelson, and J.M. Tranquada, *Rev. Mod. Phys.* **87**, 457 (2015).
121. C. Giannetti, M. Capone, D. Fausti, M. Fabrizio, F. Parmigiani, and D. Mihailovic, *Adv. Phys.* **65**, 58 (1991).
122. S. Caprara, C. Di Castro, G. Seibold, and M. Grilli, *Phys. Rev. B* **95**, 224511 (2017).
123. T.M. Rice, *Philos. Mag.* **97**, 360 (2017).
124. G. Bilbro and W.L. McMillan, *Phys. Rev. B* **14**, 1887 (1976).
125. A.M. Gabovich, M.S. Li, H. Szymczak, and A.I. Voitenko, *J. Phys.: Condens. Matter* **15**, 2745 (2003).
126. T. Ekino, A.M. Gabovich, M.S. Li, M. Pękała, H. Szymczak, and A.I. Voitenko, Symmetry **3**, 699 (2011).
127. A.M. Gabovich, M.S. Li, H. Szymczak, and A.I. Voitenko, *Phys. Rev. B* **92**, 054512 (2015).
128. G.Z. Ye, J.-G. Cheng, J.-Q. Yan, J.P. Sun, K. Matsubayashi, T. Yamauchi, T. Okada, Q. Zhou, D. S. Parker, B.C. Sales, and Y. Uwatoko, *Phys. Rev. B* **94**, 224508 (2016).
129. T. Helm, F. Flicker, R. Kealhofer, P.J.W. Moll, I.M. Hayes, N.P. Breznay, Z. Li, S.G. Louie, Q.R. Zhang, L. Balicas, J.E. Moore, and J.G. Analytis, *Phys. Rev. B* **95**, 075121 (2017).
130. S.J. Denholme, A. Yukawa, K. Tsumura, M. Nagao, R. Tamura, S. Watauchi, I. Tanaka, H. Takayanagi, and N. Miyakawa, *Sci. Rep.* **7**, 45217 (2017).
131. M.Q. Ren, Y.J. Yan, J. Jiang, S.Y. Tan, J. Miao, C. Chen, Y. Song, C.L. Zhang, P.C. Dai, B.P. Xie, T. Zhang, and D.L. Feng, *Philos. Mag.* **97**, 527 (2017).
132. J. Hartge, L. Forro, D. Mandrus, M.C. Martin, C. Kendziora, and L. Mihaly, *J. Phys. Chem. Sol.* **54**, 1359 (1993).
133. J.R. Kirtley, *Int. J. Mod. Phys. B* **4**, 201 (1990).
134. T. Hanaguri, C. Lupien, Y. Kohsaka, D.-H. Lee, M. Azuma, M. Takano, H. Takagi, and J.C. Davis, *Nature* **430**, 1001 (2004).
135. M. Vershinin, S. Misra1, S. Ono, Y. Abe, Y. Ando, and A. Yazdani, *Science* **303**, 1995 (2004).
136. K. McElroy, D.-H. Lee, J.E. Hoffman, K.M. Lang, J. Lee, E.W. Hudson, H. Eisaki, S. Uchida, and J.C. Davis, *Phys. Rev. Lett.* **94**, 197005 (2005).
137. M. Vojta, T. Vojta, and R.K. Kaul, *Phys. Rev. Lett.* **97**, 097001 (2006).
138. Y. Kohsaka, C. Taylor, K. Fujita, A. Schmidt, C. Lupien, T. Hanaguri, M. Azuma, M. Takano, H. Eisaki, H. Takagi, S. Uchida, and J.C. Davis, *Science* **315**, 1380 (2007).
139. M. Vojta and O. Rösch, *Phys. Rev. B* **77**, 094504 (2008).
140. V. Hinkov, D. Haug, B. Fauqué, P. Bourges, Y. Sidis, A. Ivanov, C. Bernhard, C.T. Lin, and B. Keimer, *Science* **319**, 597 (2008).
141. E.H. da Silva Neto, R. Comin, F. He, R. Sutarto, Y. Jiang, R.L. Greene, G.A. Sawatzky, and A. Damascelli, *Science* **347**, 282 (2015).
142. Z-X. Li, F. Wang, H. Yao, and D.-H. Lee, *Phys. Rev. B* **95**, 214505 (2017).
143. A.I. Larkin and Yu.N. Ovchinnikov, *Zh. Éksp. Teor. Fiz.* **51**, 1535 (1966) [*Sov. Phys. JETP* **24**, 1035 (1966)].
144. A.M. Gabovich, E.A. Pashitskii, and A.S. Shpigel, *Fiz. Tverd. Tela* **18**, 3279 (1976) [*Sov. Phys. Solid State* **18**, 1911 (1976)].

145. A. Barone and G. Paterno, *The Physics and Applications of the Josephson Effect*, John Wiley and Sons, New York (1982).
146. Yu.S. Barash and A.A. Svidzinskii, *Zh. Éksp. Teor. Fiz.* **111**, 1120 (1997) [*Sov. Phys. JETP* **84**, 619 (1997)].
147. T. Imaizumi, T. Kawai, T. Uchiyama, and I. Iguchi, *Phys. Rev. Lett.* **89**, 017005 (2002).
148. T. Ekino, A.M. Gabovich, M.S. Li, H. Szymczak, and A.I. Voitenko, *J. Phys.*: *Condens. Matter* **28**, 445701 (2016).
149. E.L. Wolf, *Principles of Electron Tunneling Spectroscopy*, Oxford University Press, New York (1985).
150. M. Ledvij and R.A. Klemm, *Phys. Rev. B* **51**, 3269 (1995).
151. D. Daghero, M. Tortello, P. Pecchio, V.A. Stepanov, and R.S. Gonnelli, *Fiz. Nizk. Temp.* **39**, 261 (2013) [*Low Temp. Phys.* **39**, 199 (2013)].
152. S.N. Artemenko and A.F. Volkov, *Zh. Éksp. Teor. Fiz.* **87**, 691 (1984) [*Sov. Phys. JETP* **60**, 395 (1984)].
153. A.M. Gabovich, *Fiz. Nizk. Temp.* **18**, 693 (1992) [*Sov. J. Low Temp. Phys.* **18**, 490 (1992)].
154. A.M. Gabovich and A.I. Voitenko, *J. Phys.*: *Condens. Matter* **9**, 3901 (1997).
155. Y. Noat, T. Cren, F. Debontridder, D. Roditchev, W. Sacks, P. Toulemonde, and A. San Miguel, *Phys. Rev. B* **82**, 014531 (2010).
156. I.O. Kulik and I.K. Yanson, *Josephson Effect in Superconducting Tunneling Structures*, Coronet, New York (1971).
157. Y.-M. Nie and L. Coffey, *Phys. Rev. B* **59**, 11982 (1999).
158. V.M. Krasnov, *Phys. Rev. B* **91**, 224508 (2015).
159. C. Bruder, A. van Otterlo, and G.T. Zimanyi, *Phys. Rev. B* **51**, 12904 (1995).
160. Yu.S. Barash, A.V. Galaktionov, and A.D. Zaikin, *Phys. Rev. B* **52**, 665 (1995).
161. Yu.S. Barash, H. Burkhardt, and D. Rainer, *Phys. Rev. Lett.* **77**, 4070 (1996).
162. Y.-M. Nie and L. Coffey, *Phys. Rev. B* **57**, 3116 (1998).
163. A.M. Gabovich and A.I. Voitenko, *Fiz. Nizk. Temp.* **38**, 414 (2012) [*Low Temp. Phys.* **38**, 326 (2012)].
164. A.M. Gabovich, M.S. Li, H. Szymczak, and A.I. Voitenko, *Eur. Phys. J. B* **87**, 115 (2014).
165. A.M. Gabovich, A.I. Voitenko, M.S. Li, and H. Szymczak, *Physica C* **516**, 62 (2015).
166. Yu.S. Barash, A.V. Galaktionov, and A.D. Zaikin, *Phys. Rev. Lett.* **75**, 1676 (1995).
167. T. Ekino, M. Kosugi, H. Fujii, and Y. Zenitani, *Phys. Rev. B* **53**, 5640 (1996).
168. A.I. D'yachenko, V.Yu. Tarenkov, R. Szymczak, H. Szymczak, A.V. Abal'oshev, S.J. Lewandowski, and L. Leonyuk, *Fiz. Nizk. Temp.* **29**, 149 (2003) [*Low Temp. Phys.* **29**, 108 (2003)].
169. T. Takasaki, T. Ekino, A. Sugimoto, K. Shohara, S. Yamanaka, and A.M. Gabovich, *Eur. Phys. J. B* **73**, 471 (2010).
170. A.M. Gabovich and A.I. Voitenko, *Phys. Rev. B* **75**, 064516 (2007).
171. K.K. Gomes, A. Pasupathy, A. Pushp, S. Ono, Y. Ando, and A. Yazdani, *Nature* **447**, 569 (2007).
172. K.K. Gomes, A. Pasupathy, A. Pushp, S. Ono, Y. Ando, and A. Yazdani, *Physica C* **460**, Part 1, 212 (2007).
173. T. Kato, H. Funahashi, H. Nakamura, M. Fujimoto, T. Machida, H. Sakata, S. Nakao, and T. Hasegawa, *J. Supercond.* **23**, 771 (2010).
174. A. Larkin and A. Varlamov, *Theory of Fluctuations in Superconductors*, Oxford University Press, New York (2005).
175. R.I. Rey, C. Carballeira, J.M. Doval, J. Mosqueira, M.V. Ramallo, A. Ramos-Álvarez, D. Sóñora, J.A. Veira, J.C. Verde, and F. Vidal, *Supercond. Sci. Technol.* **32**, 045009 (2019).
176. W.L. McMillan, *Phys. Rev.* **175**, 537 (1968).
177. S. Caprara, J. Biscaras, N. Bergeal, D. Bucheli, S. Hurand, C. Feuillet-Palma, A. Rastogi, R.C. Budhani, J. Lesueur, and M. Grilli, *Phys. Rev. B* **88**, 020504 (2013).
178. S. Caprara, *Supercond. Sci. Technol.* **28**, 014002 (2015).
179. J.C. Phillips, A. Saxena, and A.R. Bishop, *Rep. Prog. Phys.* **66**, 2111 (2003).
180. A.M. Gabovich and A.I. Voitenko, *Phys. Rev. B* **52**, 7437 (1995).
181. M.V. Mostovoy, F.M. Marchetti, B.D. Simons, and P.B. Littlewood, *Phys. Rev. B* **71**, 224502 (2005).
182. A.J. Achkar, X. Mao, C. McMahon, R. Sutarto, F. He, R. Liang, D. A. Bonn, W. N. Hardy, and D. G. Hawthorn, *Phys. Rev. Lett.* **113**, 107002 (2014).
183. N. Poccia, M. Lankhorst, and A.A. Golubov, *Physica C* **503**, 82 (2014).
184. E.W. Carlson, S. Liu, B. Phillabaum, and K.A. Dahmen, *J. Supercond.* **28**, 1237 (2015).
185. T. Honma and P.H. Hor, *Physica C* **509**, 11 (2015).
186. A. Shengelaya and K.A. Müller, *Europhys. Lett.* **109**, 27001 (2015).
187. T. Ekino, A.M. Gabovich, M.S. Li, M. Pekała, H. Szymczak, and A.I. Voitenko, *J. Phys.*: *Condens. Matter* **20**, 425218 (2008).

Тунельні спектри розломних контактів з надпровідної кераміки Bi2212: вплив неоднорідних розподілів параметрів порядку для *d*-хвильового куперівського спарювання та хвиль зарядової густини

T. Ekino, A.M. Gabovich, M.S. Li, H. Szymczak, A.I. Voitenko

Проведено вимірювання тунельних вольт-амперних характеристик (ВАХ) розломних контактів, виготовлених з кристалів $Bi_2Sr_2CaCu_2O_{8+\delta}$ кераміки. Показано, що отримані ВАХ мають V-подібну внутрішню щілинну область подібну до тих, які характерні для ВАХ тунельних переходів між *d*-хвильовими надпровідниками. Отримані ВАХ мають різні форми для різних переходів, але всі вони виявляють розмиті структури типу горбок-ямка поза межами внутрішньої щілинної області. Тунельний струм в *ab* площині розломних контактів розраховувався в моделі неоднорідного *d*-хвильового надпровідника з частковою діелектризацією поверхні Фермі хвилями зарядової густини (ХЗГ). Проведено усереднення тунель-

ного струму за статистичними розподілами надпровідного та ХЗГ параметрів порядку. Теоретичні результати якісно відтворюють поведінку експериментальних кривих. Зроблено висновок, що спрямованість тунелювання та статистичні розподіли обох параметрів порядку є вирішальними факторами, відповідальними за спостережувані форми ВАХ для розломних контактів, виготовлених з високотемпературних оксидів.

Ключові слова: надпровідність, хвилі зарядової густини, електронна неоднорідність, тунелювання в розломних контактах, високотемпературні оксиди.

Туннельные спектры разломных контактов из сверхпроводящей керамики Bi2212: влияние неоднородных распределений параметров порядка для *d*-волнового куперовского спаривания и волн зарядовой плотности

T. Ekino, A.M. Gabovich, M.S. Li, H. Szymczak, A.I. Voitenko

Проведено измерение туннельных вольт-амперных характеристик (ВАХ) разломных контактов, изготовленных из кристаллов $Bi_2Sr_2CaCu_2O_{8+\delta}$ керамики. Показано, что полученные ВАХ имеют V-образную внутреннюю щелевую область, подобную тем, которые характерны для ВАХ туннельных переходов между *d*-волновыми сверхпроводниками. Полученные ВАХ имеют различные формы для различных переходов, но все они обнаруживают размытые структуры типа бугорок-ямка вне внутренней щелевой области. Туннельный ток в *ab* плоскости разломных контактов рассчитывался в модели неоднородного *d*-волнового сверхпроводника с частичной диэлектризацией поверхности Ферми волнами зарядовой плотности (ВЗП). Проведено усреднение туннельного тока по статистическим распределениям сверхпроводящего и ВЗП параметров порядка. Теоретические результаты качественно воспроизводят поведение экспериментальных кривых. Сделан вывод, что направленность туннелирования и статистические распределения обоих параметров порядка являются решающими факторами, ответственными за наблюдаемые формы ВАХ для разломных контактов, изготовленных из высокотемпературных оксидов.

Ключевые слова: сверхпроводимость, волны зарядовой плотности, электронная неоднородность, туннелирование в разломных контактах, высокотемпературные оксиды.